







# Development of an Interferon-Gamma Release Assay (IGRA) to Aid Diagnosis of Histoplasmosis

 Kausik Datta,<sup>a</sup> Richard LaRue,<sup>b</sup>  Nitipong Permpalung,<sup>a</sup> Sukanya Das,<sup>c</sup>  Sean Zhang,<sup>a</sup> Seema Mehta Steinke,<sup>a,d</sup> Yuri Bushkin,<sup>c</sup> Joshua D. Nosanchuk,<sup>e</sup>  Kieren A. Marr<sup>a</sup>

<sup>a</sup>Johns Hopkins University School of Medicine, Baltimore, Maryland, USA

<sup>b</sup>Vanderbilt University Medical Center, Nashville, Tennessee, USA

<sup>c</sup>Public Health Research Institute Center, NJMS-Rutgers, Newark, New Jersey, USA

<sup>d</sup>University of Pittsburgh School of Medicine, Pittsburgh, Pennsylvania, USA

<sup>e</sup>Albert Einstein College of Medicine, Bronx, New York, USA

**ABSTRACT** Establishing diagnosis of latent and active histoplasmosis is challenging. Interferon gamma-release assays (IGRAs) may provide evidence of latent and active infection. An enzyme-linked immunospot (ELISpot) assay was developed using yeast cell lysate (YCL) antigen prepared from a representative North American *Histoplasma capsulatum* strain. Assay parameters were optimized by measuring responses in healthy volunteers with and without *Histoplasma* infection. Assay performance as an aid for diagnosing histoplasmosis was assessed in a prospective cohort of 88 people with suspected or confirmed infection, and 44 healthy controls enrolled in two centers in North America (2013 to 2018). Antigen specificity of IFN- $\gamma$  release was demonstrated using ELISpot and enzyme-linked immunosorbent assay (ELISA). Antigen-evoked, single-cell mRNA expression by memory T cells was shown using flow cytometry. The area under the receiver operating characteristic curve (AUC) was estimated at 0.89 (95% confidence interval [CI]: 78.5% to 99.9%). At optimal cutoff, sensitivity was 77.2% (95% CI: 54.6% to 92.2%) and specificity was 100% (95% CI: 89.7% to 100%). Sixteen of 44 healthy volunteers (36.4%) from a region of hyperendemicity had positive responses, suggesting detection of previously unrecognized (latent) infection. The ELISpot assay is sensitive and specific as an aid to diagnose *H. capsulatum* infection and disease, supporting proof of concept and further development.

**KEYWORDS** histoplasmosis, diagnosis, IGRA, interferon gamma release, histoplasma, immunodiagnosics

*Histoplasma capsulatum* is a soilborne fungus with worldwide distribution in regions of hyperendemicity in the Americas, Asia, and Africa (1, 2). Exposure occurs via inhalation of aerosolized microconidia, which are ingested by resident and recruited phagocytes; *in vivo*, conidia convert to a yeast that maintains intracellular viability in local lymph nodes and reticuloendothelial organs (3). Most people resolve early pulmonary symptoms, developing effective interferon gamma (IFN- $\gamma$ )-dependent Th1 cellular immunity which promotes asymptomatic latent infection and granulomatous inflammation (4). Pneumonia can become chronic, manifesting as pulmonary blebs, cavities, and bronchiolitis, and can be confused with other infections and emphysema (4). Histoplasmosis also presents after dissemination beyond the lungs, typically with insidious symptoms (e.g., fever, weight loss) and/or disease involving virtually any organ, including the central nervous system (CNS), gastrointestinal tract, and skin (5). These syndromes, collectively called “progressive disseminated histoplasmosis” (PDH), are most frequently uncovered in people who have age-related senescence or biological immunosuppression administered for cancer, autoimmunity, or transplantation (5, 6). Diagnostic test performance is variable according to clinical manifestation and timing relative to infection (7). Culture and histopathology are insensitive for all manifestations. Antigen yield is highest with

**Editor** Kimberly E. Hanson, University of Utah

**Copyright** © 2022 American Society for Microbiology. All Rights Reserved.

Address correspondence to Kieren A. Marr, kmarr@pearlrx.com, or kmarr4@jhmi.edu.

The authors declare a conflict of interest. K.A.M. reports issuance of US patent (#US-10107822-B2) describing the HistoSPOT technology, licensed by Pearl Diagnostics, Inc. (Baltimore, MD). K.D. reports employment income from Pearl Diagnostics at the time of manuscript submission. K.A.M. reports income from Pearl Diagnostics and Sfunga Therapeutics. N.P. has received grants and salary support from the Health Systems Research Institute (Thailand), the Fisher Center Discovery Program (Johns Hopkins University), the Cystic Fibrosis Foundation, the National Institutes of Health, CareDx and Merck outside the submitted work and served on the Advisory Board for Shionogi Inc and the Data Review Committee for Pulmocide Ltd. S.A.M.S. reports income from Pearl Diagnostics. Y.B. holds US (#US-10900072-B2) and EU patents (#EP3828278A1) covering FISH-Flow but reports No Income from said patents. R.L., S.D. and J.N. report no conflicts.

**Received** 31 July 2022

**Returned for modification** 25 August 2022

**Accepted** 13 September 2022

**Published** 3 October 2022

disseminated disease, especially in severely immunosuppressed people, and lowest in subacute pulmonary disease (7, 8). Despite dissemination, PDH can also be characterized by relatively low fungal burdens, especially in people without severe immunosuppression, making diagnosis by culture and antigen less sensitive (9–11).

Antibody assays supplement the use of antigen assays and are useful for detecting both active and latent disease. However, performance is variable based on time after acute infection, methods used, and immunosuppression. After *Histoplasma* infection, antibody levels typically become detectable within 3 to 6 weeks of acute infection and then decline to undetectable within 1 to 3 years in the absence of recurrent exposure (9, 10). Only about 1/4 of asymptomatic people have low-level antibodies detectable in regions of endemicity, dependent on recurrent exposures, testing methods, and population immunocompetence (9, 10). Predictably, serologic sensitivity is low in people with severe immunosuppression, as well as in those with advanced HIV or organ transplantation (9, 12). Serologic testing can contribute to antigen and culture-based testing, especially for subacute and chronic disease in relatively immunocompetent people, supporting current recommendations to perform broad antigen and serologic testing when histoplasmosis is considered (9, 13–15). However, low sensitivity and limited duration of positivity limits the diagnostic utility of serology, either as an aid to diagnose active histoplasmosis or to rule out histoplasmosis in distinguishing potentially 'benign' processes, such as mediastinal masses (12, 16).

Unlike for tuberculosis (TB), no skin tests to measure hypersensitivity are commercially available; diagnosis of latent histoplasmosis is unreliable (10). Because chronic disease also presents with atypical, inflammatory, nonpulmonary manifestations, these cases frequently become apparent incidentally, with significant diagnostic delay (17). Recent reports have recognized that clinical manifestations of PDH, including fever, hepatosplenomegaly, pulmonary lesions, and pancytopenia, overlap with those of other infections (especially TB), focusing their attention on delayed diagnosis and poor outcomes; a study by the Centers for Disease Control (CDC) associated diagnosis delays of >6 weeks with poor outcomes (17). Reactivation during immunosuppression as 'surprise diagnoses' have been reported in diverse underlying conditions, including presumed autoimmune or inflammatory syndromes (e.g., inflammatory bowel disease, hemophagocytic lymphohistiocytosis), sarcoidosis, chronic lung disease, pulmonary nodules, and recently, COVID-19 (6, 17–19).

We hypothesized that relative preservation of central memory T cell responses might support the potential utility of T cell-assisted diagnostics for latent and active histoplasmosis, as with serology. Documentation of antigen-specific memory T cells could facilitate differential diagnosis and detection of latent infection, functioning similarly to current interferon-gamma release assays (IGRA) used for tuberculosis. To this end, we developed an enzyme-linked immunospot (ELISpot) assay, which we call "histoSPOT." Here, we describe validation studies using healthy donors and proof of concept of histoSPOT as an aid to diagnose histoplasmosis in people enrolled at two North American medical centers.

## MATERIALS AND METHODS

**Feasibility and proof of concept study design.** Feasibility testing was first performed on one healthy donor with a known history of latent histoplasmosis; responses from this donor were measured to compare responses to different *H. capsulatum* strain antigen concentrations and exposure times and peripheral blood mononuclear cell concentrations (PBMC), as well as to determine reproducibility in one subject over time. This adult, immunocompetent, asymptomatic volunteer was infected with *H. capsulatum* in adolescence, with nodules and calcifications persisting on pulmonary imaging. Another asymptomatic, immunocompetent volunteer treated for PDH provided blood for confirmatory testing and to validate responses using intracellular cytokine staining.

After testing these immunocompetent volunteers, we measured responses in a cohort of immunosuppressed people with suspected or confirmed acute and chronic histoplasmosis enrolled at Johns Hopkins University (JHU, Baltimore, MD), and in healthy people residing in a region of endemicity at Vanderbilt University (VAN; Nashville, TN, Fig. 1). Studies were approved by respective Institutional Review Boards and subjects consented to single or sequential blood collection. Clinical data were collected, and diagnoses were adjudicated by clinicians blinded to histoSPOT results. No disease, or 'possible,' 'probable,' and 'proven' histoplasmosis, were defined using modifications of the definitions recommended by the European Organization for Research and Treatment of Cancer/Mycoses Study Group (EORTC/MSG) (20). Proven histoplasmosis disease was defined as signs and symptoms with culture or histopathology. Probable histoplasmosis disease was defined as signs and symptoms with positivity of commercial antigen test (blood and/or urine); positive antibody titers of  $\geq 1:8$  were accepted as evidence

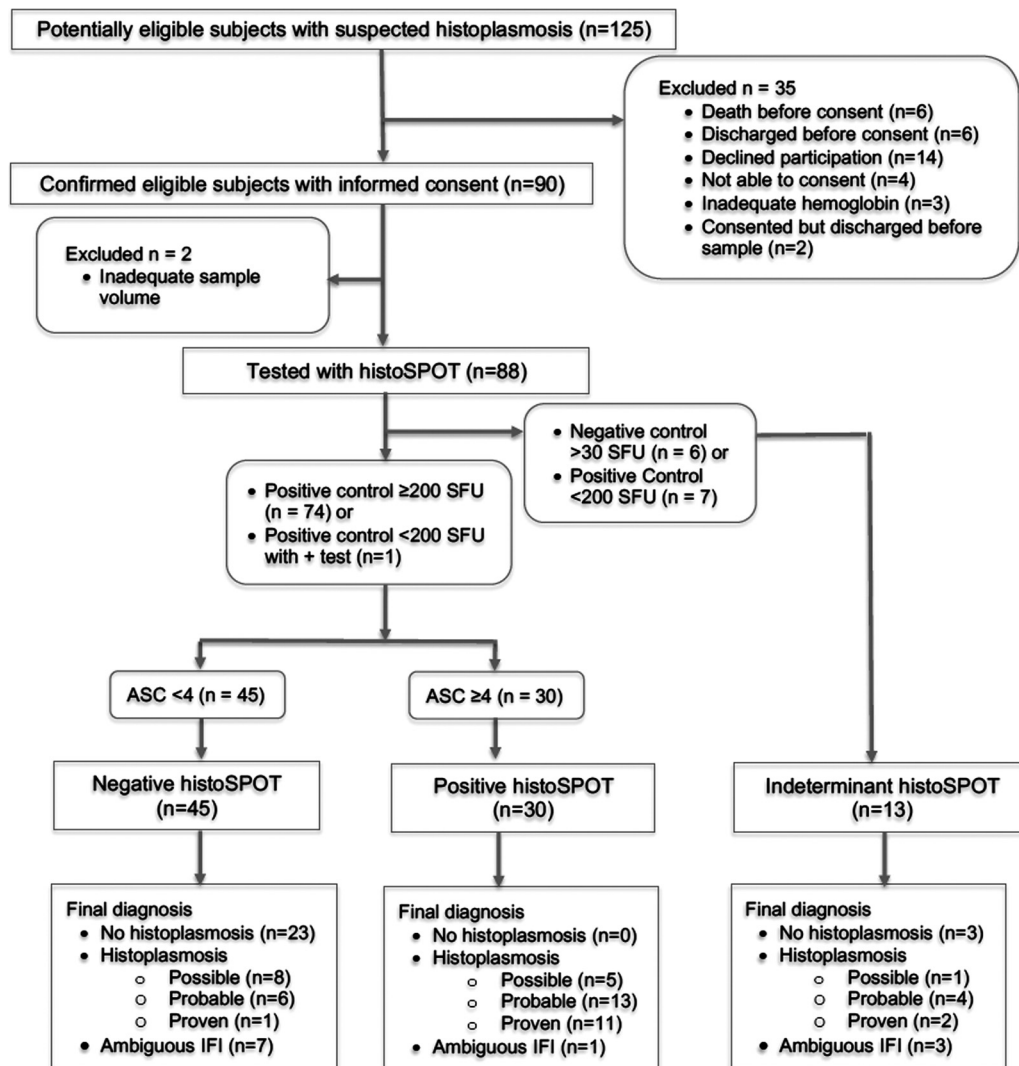


FIG 1 STARD flow diagram of subject enrollment and adjudicated diagnoses. IFI, invasive fungal infection.

for probable histoplasmosis, as in recent CDC surveillance efforts (21). Possible histoplasmosis disease included clinical signs and symptoms without microbiologic confirmation by any of the above-described tests. Asymptomatic, healthy controls with documented prior histoplasmosis using CDC criteria were considered to have “proven” latent histoplasmosis (21); asymptomatic people with known endemic exposure and history of pulmonary disease and documented pulmonary residua, with or without measurable antibodies, were considered to have “probable” latent histoplasmosis. All others, including people with alternative diagnoses, were considered “controls.” HistoSPOT assays were performed and interpreted by personnel unaware of clinical designations.

**Histoplasma yeast cell lysate antigen.** Yeast cell lysate (YCL) antigens were prepared using North American *H. capsulatum* strain G217B, representing chemotype NAM2, now called *H. ohioensis*; and G168A, representing Nam1, now called *H. mississippiensis* (22). Yeasts were grown to yeast phase in supplemented Ham’s F12; yeast cells were pelleted, and lysate was produced by shearing under liquid nitrogen. Yeast cell lysates were diluted in phosphate-buffered saline (PBS) with phosphatase inhibitor cocktail, stored in aliquots at  $-80^{\circ}\text{C}$ , and  $0.22\text{-}\mu\text{m}$  filter-sterilized prior to use. Protein concentrations were measured with a bicinchoninic acid assay (Pierce/Thermo Fisher Scientific).

**Interferon-gamma release assays.** Blood drawn from healthy, asymptomatic volunteers and people with suspected or confirmed histoplasmosis was processed to peripheral blood mononuclear blood cells (PBMCs) using Lymphocyte Separation Medium (Lonza), within 2 h of blood draw. Blood drawn from distant sites (Tennessee) was transported by overnight transport to enable PBMC processing within 12 to 24 h. PBMCs were either stored frozen in liquid nitrogen and thawed prior to use or tested immediately after preparation; each run included mitogen-containing controls to ensure validity, as detailed below.

Two healthy volunteers with known latent pulmonary histoplasmosis provided blood samples to develop and optimize assay parameters. IFN- $\gamma$  secretion was measured by enzyme-linked immunosorbent assay (ELISA) and ELISpot after co-incubating PBMCs with antigen ( $10\text{ }\mu\text{g/mL}$  YCL) or mitogen ( $2.5\text{ }\mu\text{g/mL}$  phytohemagglutinin [PHA], Sigma) in complete culture medium (RPMI 1640 with 10% vol/vol heat-inactivated fetal bovine

serum; Mediatech/Corning) for 48 h. ELISAs were performed with IFN- $\gamma$  ELISA kits (Invitrogen/Thermo Fisher). ELISpot assays were performed using the Human IFN- $\gamma$  ELISpot<sup>PRO</sup> assay kit with alkaline phosphatase (ALP)-conjugated detection antibody (Mabtech). Spot-forming units (SFU) were analyzed and counted with a BioReader 4000 Pro-X with BIOSYS software (BioSys GmbH, Karben, Germany). Control wells containing no antigen (negative control) and mitogen (positive control) were included with every run.

**Intracellular cytokine staining by FISH-Flow.** Cytokine mRNA production by T cells was measured using flow-cytometry ("FISH-Flow"), as previously described (23). PBMCs from cases and controls were stimulated in complete culture medium supplemented with co-stimulatory anti-CD28 and CD49d MAb (monoclonal antibodies; all Abs from BD Biosciences) alone (control) or 10  $\mu$ g/mL YCL. mRNA targets were measured after 6-h stimulation. After incubation, PBMCs were phenotyped with anti-CD3-FITC (fluorescein isothiocyanate) and anti-CD45RO-PE MAb on ice. Immunostained cells were fixed and permeabilized and hybridized with custom Cy5-labeled single molecule-FISH probe sets against cytokine and chemokine mRNAs (LGC Biosearch Technologies) as previously described (23). CD3<sup>+</sup> and CD3<sup>+</sup> cells were gated using SSC-A and FITC channel, and the PE channel on the CD3<sup>+</sup> population was used to gate CD45RO<sup>+</sup> T cells. A total of 200,000 events per sample were analyzed.

**Analyses.** Results are represented quantitatively as mean antigen (Ag)-specific spot-forming units (SFU) per 10<sup>5</sup> PBMC, with subtraction of background control (No Ag) wells (Adjusted Spot Counts, ASC). Individual group comparisons of central tendencies were done by Student's *t* test (mean) or Mann-Whitney U test (median) as appropriate; multiple comparisons of group means were done by one-way (for single variable) or two-way (for dual variables) analysis of variance (ANOVA) with Tukey's *post hoc* test. All statistical analyses, including Receiver Operator Characteristic (ROC) curves, sensitivity, specificity, and likelihood ratios, were performed using GraphPad Prism v9.4.1 for Windows (GraphPad Software, La Jolla, CA). Clinical performance (sensitivity, specificity, positive and negative predictive values) of HistoSPOT in the overall cohort was calculated with MedCalc (v.20.114).

## RESULTS

**Assay development.** In development, responses were measured after varying antigen, PBMC concentrations, and incubation timing. ELISA was performed to first establish whether IFN- $\gamma$  was secreted in response to *H. capsulatum* YCL from strain G217B, using PBMC from one volunteer known to be infected (Fig. 2A). Results demonstrated IFN- $\gamma$  secretion in response to YCL, but with lower yield at high concentration. Yeast cell lysate at 10  $\mu$ g/mL produced sustained and time-graded IFN- $\gamma$  secretion over 24 and 48 h (adjusted *P* < 0.038 compared to 6 h, two-way ANOVA with Tukey's test). Further experiments were performed using 10  $\mu$ g/mL YCL, which produced higher IFN- $\gamma$  levels compared to No Ag at 24 and 48 h (*P* < 0.014, one-way ANOVA with Tukey's test). With a 48-h exposure of PBMCs to 10  $\mu$ g/mL YCL, the spot-forming units (SFU) were optimal with inputs of both 10<sup>5</sup> and 2  $\times$  10<sup>5</sup> PBMCs. Considering that PBMC counts are probably limited in immunosuppressed people, the lower count of 1  $\times$  10<sup>5</sup> PBMCs per well was chosen as the input for HistoSPOT (Fig. 2B). Figure 2C demonstrates clear and quantifiable SFU using these conditions with PBMC from the same healthy volunteer with known infection. ELISpot responses were compared using YCL prepared from both North American strains (G217B and G186A) in 21 subjects with proven/probable/possible histoplasmosis enrolled at JHU, revealing some quantitative differences (Fig. 2D); for each subject, a G186A response corresponded with a G217B response, but with lower mean spot counts (SFU 36 versus 21, respectively; *P* < 0.017, paired *t* test). Further studies used YCL from G217B, representative of NAM2, the most prevalent strain in North America (22). Based on these studies, subsequent assays were performed using 10<sup>5</sup> PBMCs per well, provided mitogen responses were adequate (as detailed below), with 48 h of antigen exposure prior to spot development. The stability of responses over time was measured in one healthy volunteer who provided multiple blood draws over a 4-year period; in this subject, IFN- $\gamma$  spots were consistently present, but quantitatively variable (Fig. 2E).

To validate the results of ELISpot and ELISA, both of which measure secreted protein, IFN- $\gamma$  mRNA was measured using intracellular staining with flow cytometry (FISH-Flow) (23). Responses from the same representative healthy (previously infected) volunteer (Case 1), an otherwise healthy patient previously treated for PDH (Case 2), and a healthy (uninfected) control are shown in Fig. 3A. Frequency estimates for numerous cytokine mRNAs are summarized in the table (Fig. 3B). *Histoplasma* YCL antigen stimulation induced pro-inflammatory cytokine responses with IFN- $\gamma$  and tumor necrosis factor alpha (TNF- $\alpha$ ) in both cases, but not in the uninfected control. Both cases also had modest increases in interleukin (IL)-2 and IL-17; YCL antigen also stimulated mRNA for IL-2 in the healthy noninfected control. CD3<sup>+</sup> subset profiles were measured from Case 2, who had been treated for PDH within the

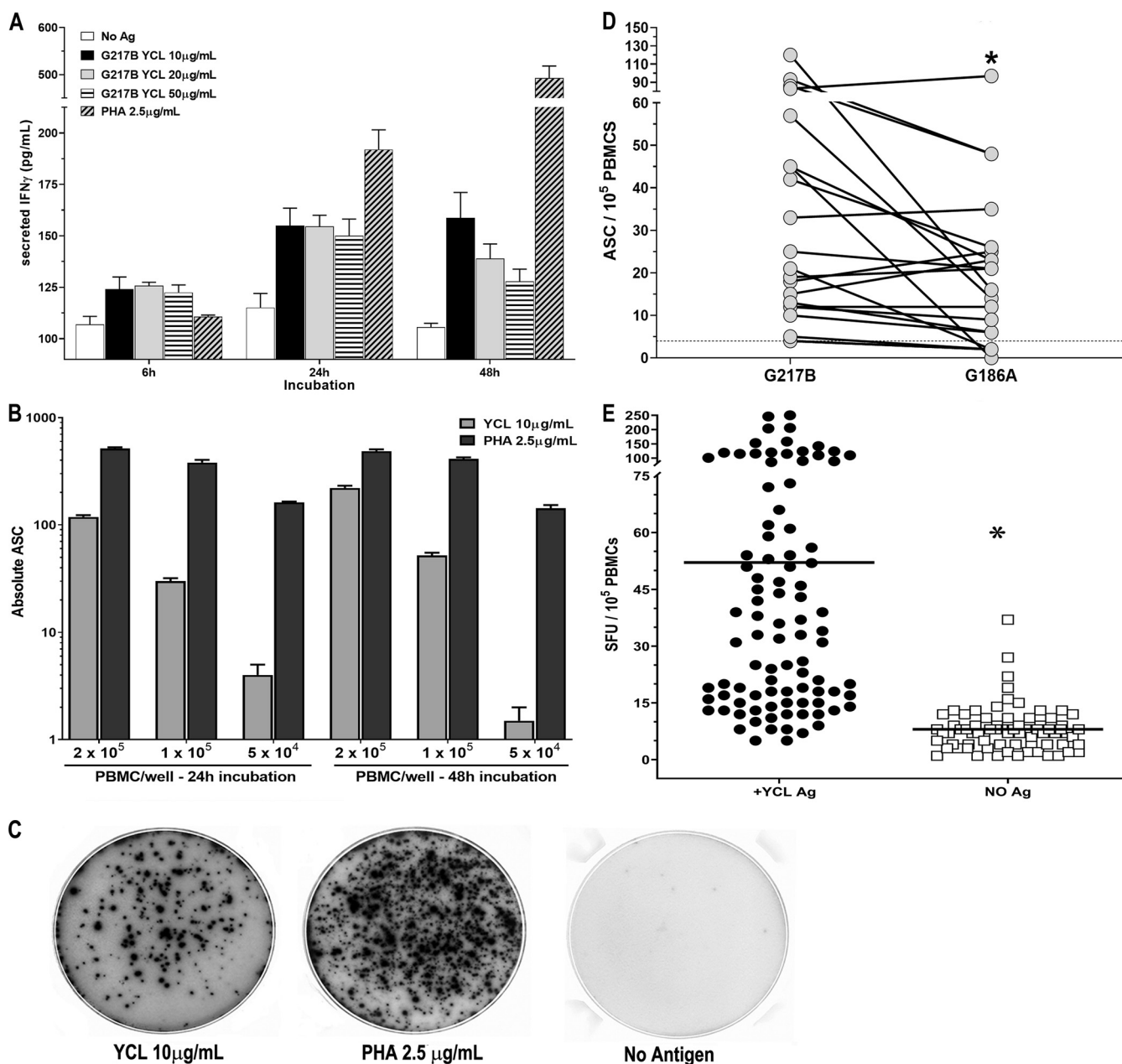
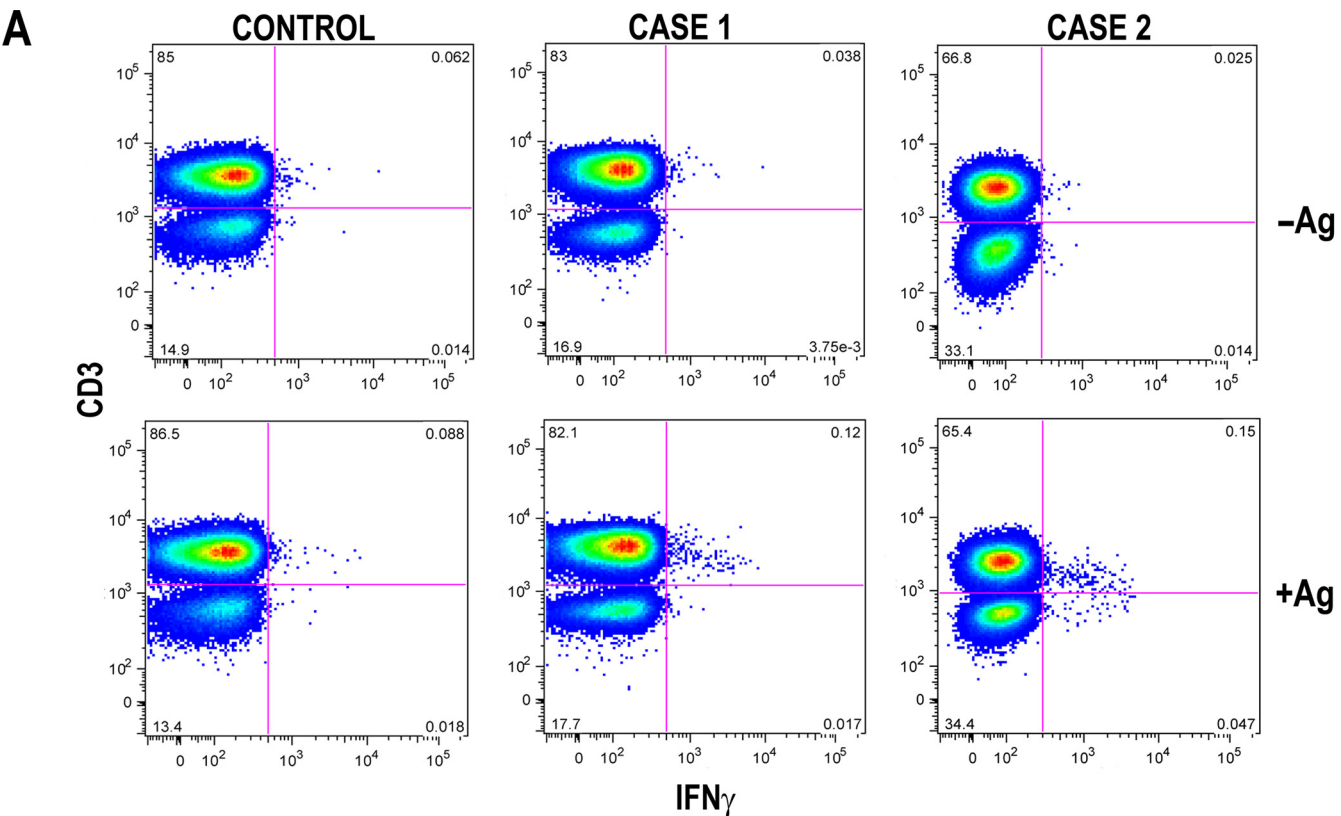


**FIG 2** Optimizations of assay conditions. (A) Interferon (IFN)- $\gamma$  (measured by enzyme-linked immunosorbent assay [ELISA], mean of 4 replicate wells from 2 independent assays) secreted in response to different antigen or mitogen concentrations at different incubation times by peripheral blood mononuclear cells PBMCs from one healthy volunteer case. (B) Quantitative histoSPOT responses measured using different PBMC inputs and antigen exposure times, using PBMCs from the same healthy volunteer in three different experiments. (C) Representative IFN- $\gamma$  spot appearance in histoSPOT wells in response to G217B YCL and phytohemagglutinin (PHA) mitogen. (D) histoSPOT responses in 21 subjects with proven/probable/possible histoplasmosis, comparing two North American strains; \*,  $P < 0.017$ ; paired  $t$  test. Dotted line represents ASC 4, the cutoff ASC for G217B YCL. (E) HistoSPOT responses of one subject tested over 4 years. \*,  $P < 0.001$ ; Mann-Whitney U test.

past year. In this case, YCL antigen-reactive T cells expressing IFN- $\gamma$ , IL-2, TNF- $\alpha$ , and IL-17A, analyzed by FISH-Flow, were clearly within the memory CD3 $^{+}$ CD45RO $^{+}$  subset; the latter accounting for 55% to 85% of the observed reactivity (data not shown).

**Proof-of-concept testing and performance characteristics.** Demographics and clinical characteristics of subjects approached and enrolled in the study are summarized in Table 1. The age range was wide, and enrollment represented varied geographic exposures. Underlying diseases reflected varied conditions, including none recognized. Histoplasmosis was the most common adjudicated diagnosis from the episode that triggered subject enrollment.





**B**

|               | Control |       | Case #1 |       | Case #2 |       |
|---------------|---------|-------|---------|-------|---------|-------|
|               | -Ag     | +Ag   | -Ag     | +Ag   | -Ag     | +Ag   |
| IFN $\gamma$  | 0.062   | 0.088 | 0.038   | 0.12  | 0.025   | 0.15  |
| IL-2          | 0.028   | 0.077 | 0.027   | 0.11  | 0.028   | 0.087 |
| TNF- $\alpha$ | 0.021   | 0.009 | 0.005   | 0.072 | 0.018   | 0.076 |
| IL-17         | 0.069   | 0.038 | 0.075   | 0.17  | 0.037   | 0.062 |

**FIG 3** Cytokine mRNA production after antigen (or no-antigen) control using FISH-Flow. (A) Representative flow cytometric distribution of IFN- $\gamma$  mRNA producing CD3<sup>+</sup> T cells from one healthy control and two histoplasmosis cases. Case 1 is the same healthy case shown in Fig. 2; Case 2 is a recently diagnosed and treated, otherwise healthy man with progressive disseminated histoplasmosis (PDH). (B) Frequency of cells expressing IFN- $\gamma$ , IL-2, tumor necrosis factor alpha (TNF- $\alpha$ ), and IL-17 mRNAs after control and Ag exposure from healthy control, cases 1 and 2. Data are expressed as % of total events captured in gate and are extracted from 1 experiment representative of 2 performed.

Fig. 4A and B show frequency histograms for positive (PHA) and negative (no-antigen) controls from within the JHU cohort. Responses show appropriate skewing. With this distribution, the lower limit to accept a positive control was established at 200 SFU, and the highest limit to accept a negative control was set at 30 SFU.

Spot responses from 79 subjects enrolled at JHU with proven ( $n = 13$ ), probable ( $n = 9$ ), and possible ( $n = 23$ ) histoplasmosis, and 34 controls, were used to draw ROC curves (Fig. 5). Thirteen subjects with indeterminate SFU responses (based on limits above) were excluded from analyses. Figure 5A depicts a case as proven or probable histoplasmosis and Fig. 5B includes suspected infection (possible) in the case definition. ROC curves showed good predictability, with an estimated AUC of 0.89. Likelihood ratios were maximal ( $\geq 26.2$ ) using the cutoff of 4 ASC, where the sensitivity was 77.3% (95% confidence interval [CI]: 54.6% to 92.2%) and specificity was 100% (95% CI: 89.7% to 100%). Inclusion of suspected histoplasmosis as a

**TABLE 1** Demographics and clinical characteristics of study subjects ( $n = 88$ )<sup>a</sup>

| Characteristic   | N (%) <sup>b</sup> |
|--|--------------------|
| Gender (male) <sup>c</sup>                             | 55 (64.7)          |
| Age (yrs), median (range) <sup>c</sup>                 | 54 (9–91)          |
| Race <sup>c</sup>                                      |                    |
| White  | 68 (80)            |
| Black/African-American                                 | 11 (12.9)          |
| Asian  | 6 (7.1)            |
| Hispanic ethnicity <sup>c</sup>                        | 6 (7.1)            |
| Region of endemicity                                   |                    |
| Southeast U.S.   | 48 (54.5)          |
| Northeast U.S.   | 16 (18.2)          |
| Midwest U.S.   | 5 (5.7)            |
| Rocky Mountain U.S.                                    | 1 (1.1)            |
| Southwest U.S.   | 1 (1.1)            |
| Central or South America                               | 9 (10.2)           |
| Unknown  | 8 (9.1)            |
| Underlying condition <sup>d</sup>                      |                    |
| Hematological malignancy                               | 22 (25)            |
| Solid organ transplant                                 | 20 (22.7)          |
| Autoimmune/immunologic                                 | 11 (12.9)          |
| HIV/AIDS   | 4 (4.5)            |
| Solid tumor  | 4 (4.5)            |
| Pulmonary disease                                      | 4 (4.5)            |
| None   | 20 (23.5)          |
| Other  | 3 (3.5)            |
| Absolute lymphocyte count, median (range) <sup>c</sup> | 690 (0–6,470)      |
| Diagnosis <sup>e</sup>                                 |                    |
| Histoplasmosis, proven                                 | 14                 |
| Histoplasmosis, probable                               | 23                 |
| Histoplasmosis, possible                               | 14                 |
| Aspergillosis, proven or probable                      | 8                  |
| Cryptococcosis, proven                                 | 1                  |
| Possible IFI, NOS                                      | 10                 |
| No IFI, other  | 15                 |
| Mixed infections                                       | 3                  |
| Histoplasmosis classification                          |                    |
| Subacute pulmonary                                     | 12                 |
| Progressive disseminated                               | 21                 |
| Chronic pulmonary                                      | 8                  |
| Latent   | 7                  |

<sup>a</sup>IFI, invasive fungal infection.<sup>b</sup>Data are given as n (%) unless otherwise specified.<sup>c</sup>Excludes data from 3 subjects for whom demographic information was unavailable.<sup>d</sup>Autoimmune/immunologic conditions include rheumatoid arthritis ( $n = 1$ ), idiopathic CD4 lymphopenia ( $n = 1$ ), common variable immunodeficiency ( $n = 1$ ), mixed connective tissue disorder ( $n = 1$ ), myasthenia gravis ( $n = 1$ ), and pauci-immune crescentic glomerulonephritis ( $n = 1$ ). Solid organ transplant includes kidney ( $n = 10$ ), liver ( $n = 5$ ), lung ( $n = 2$ ), heart ( $n = 2$ ), and mixed kidney/liver ( $n = 1$ ). Pulmonary disease includes asthma ( $n = 1$ ), bronchiectasis ( $n = 1$ ), cystic fibrosis ( $n = 1$ ), and sarcoidosis ( $n = 1$ ). Other includes Ehlers Danlos syndrome ( $n = 1$ ), end-stage liver disease ( $n = 1$ ), and congenital heart disease ( $n = 1$ ).<sup>e</sup>No IFI, other adjudicated diagnoses include: no definitive diagnosis ( $n = 4$ ), allergic bronchopulmonary aspergillosis ( $n = 1$ ), hemophagocytic lymphohistiocytosis ( $n = 1$ ), probable sarcoidosis ( $n = 2$ ), cytomegalovirus disease ( $n = 1$ ), *Helicobacter pylori* infection ( $n = 1$ ), Chikungunya virus infection ( $n = 1$ ), meningoencephalitis NOS ( $n = 1$ ), bacterial sepsis ( $n = 2$ ), and nocardiosis ( $n = 1$ ). Mixed infections include possible mixed IFI + mycobacterial infection ( $n = 2$ ) and mixed cryptococcosis + histoplasmosis ( $n = 1$ ).

case (Fig. 5B) predictably decreased the AUC (0.82), reducing sensitivity to 64.4% (95% CI: 48.8% to 78.1%) with no change in specificity. The cohort also included 24 subjects who were confirmed to have other invasive fungal infections (cryptococcosis, aspergillosis, and pneumocystosis); no false-positives occurred using the cutoff of 4 ASC. Correlating positive and negative

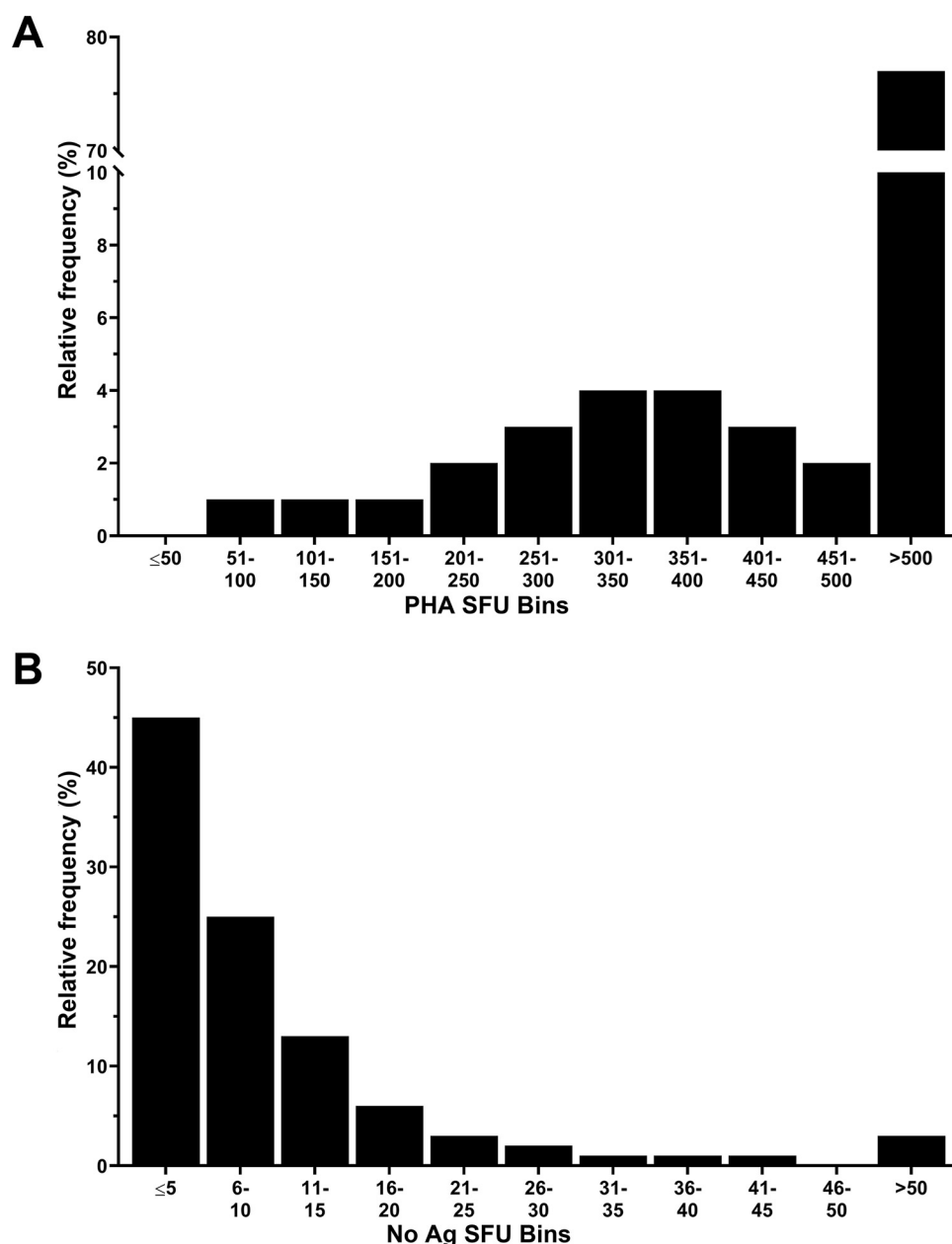


**FIG 4** Frequency histograms of spot-forming units (SFUs) in control enzyme-linked immunospot (ELISpot) wells containing mitogen (PHA, 2.5  $\mu$ g/mL) (A) and no antigen (B). Assay acceptance cutoffs of PHA  $\geq$  200 SFUs and No Antigen  $\leq$  30 SFUs based on the frequencies were incorporated into the assay algorithm.

predictive values (PPV, NPV) are variable as predicted by pre-test probability of disease. Assuming pre-test probability ranging from 20% to 60% in regions of low and high endemicity, PPV would be at 100% and NPV would vary from 74.6% (95% CI: 57.6% to 86.4%, at 60% pre-test probability) to 94.6% (95% CI: 89.1% to 97.4%, at 20% pre-test probability).

Assay results were analyzed separately in 44 healthy controls enrolled at VAN in Tennessee, a region of high endemicity. Sixteen (36.4%) healthy controls from Tennessee had positive responses at the cutoff of 4 ASC, suggesting unrecognized, latent infection. The composite performance using data from all subjects with suspected and confirmed infection and healthy controls residing in different regions of endemicity (JHU and VAN) using the ROC-derived cutoff of 4 SFU was 80% (95% CI: 59.3% to 83.2%) sensitivity and 79.3% (95% CI: 68.5% to 87.6%) specificity.



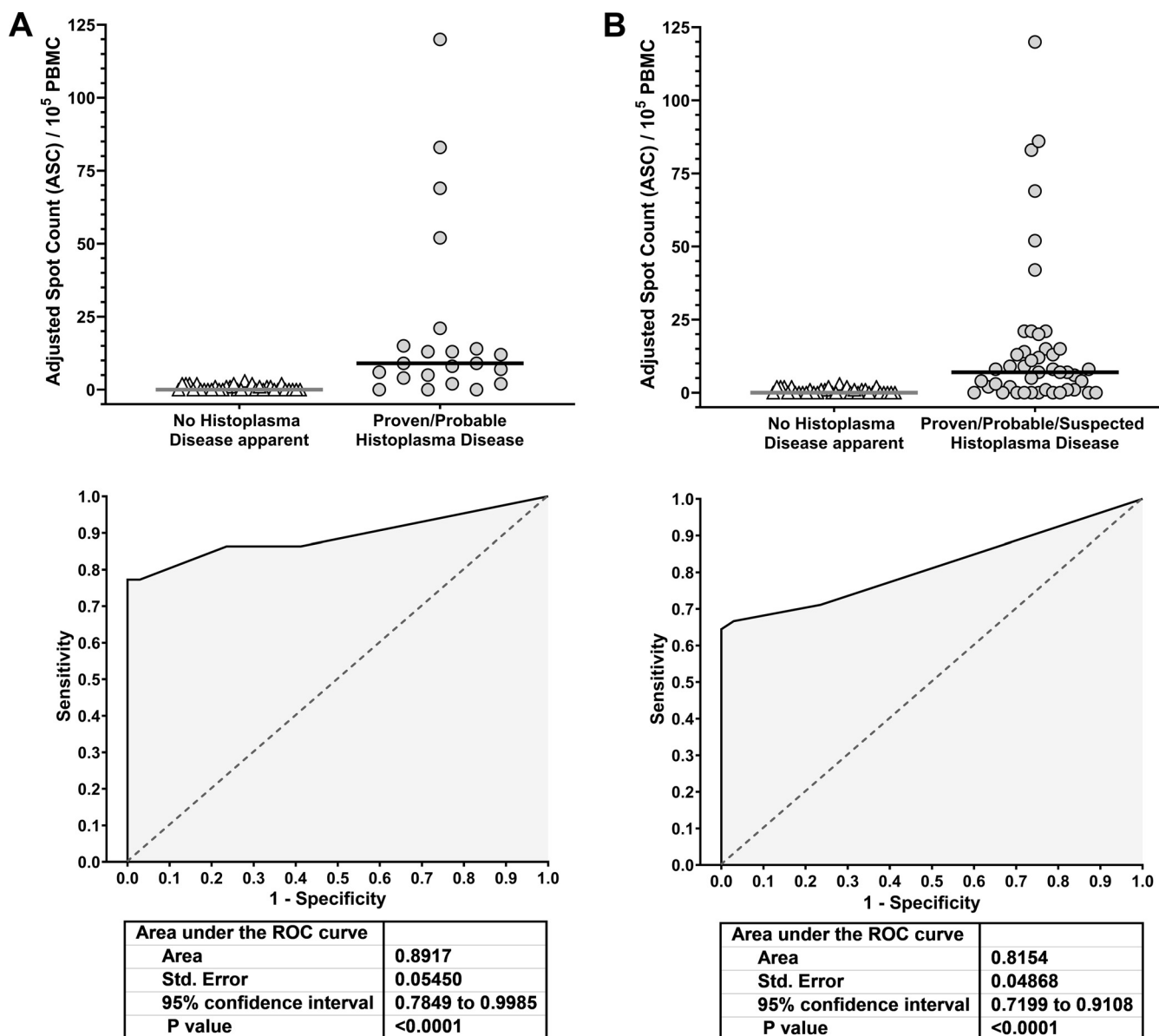


**FIG 5** Receiver operator characteristics (ROC) curves drawn from subjects in the Johns Hopkins University (JHU) cohort, with case definitions including either Proven/Probable infection (A) or Proven/Probable and Suspected Histoplasma infection (B). Spot distributions and computed performance values based on different cutoffs are as shown.

**Representative proven or probable histoplasmosis cases.** Representative cases provide additional information on potential utility of histoSPOT as an aid for diagnosing different forms of histoplasmosis. Table 2 summarizes results among cases with proven and probable histoplasmosis, with several subjects having multiple tests performed over time. Although YCL-specific spot counts are seen in many cases with proven disease, negative results are apparent in some patients, especially those with severe immunosuppression. Serial sampling showed responses that increased over time and with successful treatment. An illustrative case is Subject 8, a man from El Salvador who underwent haploidentical bone marrow transplant (BMT) and shortly afterward developed pulmonary nodules with fever and fungal markers suggestive of an invasive fungal infection. At the time of first sampling, his histoSPOT assay result was indeterminate with a low (<200 SFU) mitogen response. Follow-up testing after 4 months of antifungal treatment showed positive results. His brother, who was his stem cell donor, also had a positive histoSPOT result, potentially consistent with shared geographic exposure from

**TABLE 2** Representative cases with proven or probable histoplasmosis<sup>a</sup>

| Subject | Underlying disease  | Clinical presentation   | Histo Ag | Histo Ab        | Other Ag   | Culture and pathology                           | Therapy                       | Diagnosis                             | HistoSPOT result <sup>b</sup>               |
|---------|---|---|----------|-----------------|--|---|-------------------------------|---------------------------------------|---|
| 1       | Kidney transplant   | Swollen ankle   | Positive | NA              | NA   | Joint fluid culture +<br><i>H. capsulatum</i>   | Amphotericin,<br>itraconazole | Proven disseminated<br>histoplasmosis | ASC = 45                                    |
| 2       | None  | Pulmonary nodules   | Positive | Negative        | NA   | NA  | Itaconazole                   | Probable pulmonary<br>histoplasmosis  | ASC = 15                                    |
| 3       | Rheumatoid arthritis                                      | Bronchiectasis and fibrotic changes<br>on CT chest                                | Positive | Positive (1:8)  | NA   | NA  | Itaconazole                   | Probable pulmonary<br>histoplasmosis  | ASC = 10                                    |
| 4       | HIV/AIDS  | Respiratory distress  | Positive | Negative        | $\beta$ DG+ (366)                                | BAL fluid culture +<br><i>H. capsulatum</i>     | Itaconazole                   | Proven pulmonary<br>histoplasmosis    | ASC = 12                                    |
| 5       | None  | Oral lesions  | Positive | NA              | NA   | Pathology and culture +<br><i>H. capsulatum</i> | Itaconazole                   | Proven disseminated<br>histoplasmosis | ASC = 8                                     |
| 6       | AML   | Pulmonary nodules, neutropenic<br>fever   | Positive | NA              | GM EIA+ (0.5)                                    | NA  | Amphotericin,<br>posaconazole | Probable pulmonary<br>histoplasmosis  | To = IND;<br>T + 1 wk = 6                   |
| 7       | No significant<br>medical history                         | Fatigue, arthralgias, sweats,<br>pulmonary nodules eosinophilia,<br>arachnoiditis | Negative | Positive (1:32) | $\beta$ DG- (58), GM EIA-<br>(0.05)              | NA  | Itaconazole                   | Probable PDH                          | To = 64; T + 1 yr =<br>140; T + 2 yr = 7    |
| 8       | HIV, lymphoma, s/p<br>BMT                                 | Pulmonary nodules, myalgias, fever  | Positive | Negative        | $\beta$ DG- (48)                                 | Lymph node<br>non-necrotizing<br>granulomas     | Amphotericin,<br>posaconazole | Probable pulmonary<br>histoplasmosis  | To = 2;<br>T + 3 mo = 38;<br>BMT donor = 15 |
| 9       | Systemic sclerosis  | Pneumonia, bone marrow and liver<br>dissemination                                 | Positive | Negative        | NA   | Pathology + liver,<br>bone marrow               | Itaconazole                   | Proven disseminated<br>histoplasmosis | To = 6; T + 1 yr = 5                        |
| 10      | Pancreatic carcinoma,<br>treatment-related<br>lymphopenia | Scattered patchy and speculated<br>consolidation, fever, diarrhea                 | Positive | Negative        | BAL fluid GM EIA +<br>(1.4), $\beta$ DG NEG (44) | Pathology +<br>granulomas lung                  | Posaconazole                  | Probable pulmonary<br>histoplasmosis  | To = IND;<br>T + 3 mo = 21                  |

<sup>a</sup>Ag, antigen; Ab, antibody; NA, not applicable;  $\beta$ DG, commercial  $\beta$ -D-glucan assay; BAL, bronchoalveolar lavage; GM EIA, Galactomannan Enzyme Immunoassay; IND, indeterminate based on positive and/or negative-control results; BMT, bone marrow transplant. Commercial diagnostic assay results include *Histoplasma* Ag and Ab,  $\beta$ DG, and GM EIA, with corresponding numeric values representing reported results.

<sup>b</sup>ASC = adjusted spot count (mean Ag spots - mean No-Ag spots) for histoSPOT assay; To = time of presentation; T = day of presentation + corresponding time afterwards.

a region of high endemicity. The observation of increased spot count over time could also be consistent with transferred cellular immunity. Similar conversion from indeterminate to positive results following treatment were seen in multiple other subjects.

## DISCUSSION

Histoplasmosis has been increasingly reported in the United States, especially in people with biological immunosuppression (17, 24, 25). The organism is difficult to culture, and fungal burden is variable to low, dependent on the host and disease state (26–28). We hypothesized that an IGRA could help to diagnose latent *H. capsulatum* infection and risk-stratify in the setting of active disease, especially in people with relatively preserved cellular immunity; results from two cohorts living in different areas of endemicity in the United States demonstrate proof of concept for an IGRA that uses sensitive and quantitative ELISpot technology.

The clinical presentations of histoplasmosis can be varied, extending well beyond the classic pulmonary syndrome to include fever of unknown origin, gastrointestinal and mouth lesions, granulomatous hepatitis, duodenitis, migratory arthritis, vasculitic skin rashes, and CNS disease, to name a few (25, 29–39). Frequently, these manifestations are not recognized as histoplasmosis, leading to diagnostic delay and misdiagnoses. Infection can evolve and present with subacute or chronic symptomatology, especially in elderly patients and those with immunosuppression caused by biological therapies (e.g., transplant, autoimmune disease, and cancer) (6, 40). Establishing a diagnosis of histoplasmosis in varied settings can be challenging, both in regions of endemicity and regions of non-endemicity. One US study reported that only 33% of diagnoses were supported with lab tests (17). Antigen tests have low sensitivity with subacute syndromes, estimated at 30% in a recent review (7, 9, 11). In a large cohort of HIV-infected patients prospectively enrolled in Brazil, the sensitivity of urine antigen testing was estimated at only 71% (11). Latent infection is difficult to detect; unlike for TB, no skin tests to measure hypersensitivity exist, and antibody detection is insensitive and temporal, with levels waning to undetectable within a few years after infection (10). Given the limitations of both antigen and antibody testing, the current recommendation is to test both antigen and antibody in settings of suspected disease (41), with antibody responses assisting in evaluation of relative risks as evidence of prior (latent) infection. IGRAs can be a useful diagnostic adjunct, providing similar diagnostic risk stratification based on immunoreactivity and, potentially, to minimize false diagnoses conferred by antigen cross-reactivity (7). Support for this was demonstrated using ELISA to detect latent infection in healthy people residing in Colombia, with crude yeast and mycelial antigen preparations stimulating IFN- $\gamma$  production (42).

In this study, the histoSPOT assay was 78% sensitive and 100% specific as an aid for diagnosing histoplasmosis in people with suspected active disease. While this is not evidence of definitive disease (as with culture or histopathology), recognition of prior infection can assist differential diagnosis in disease states which are characterized by low fungal burden and low likelihood of culture recovery (17, 24). Evaluation of cases suggests that sensitivity may be suppressed with immunosuppression, especially low lymphocyte counts. As with other IGRAs, interpretation of results requires consideration of pre-test probability of disease, a complex function of host immunosuppression, geographic exposure, and clinical presentation. With the performance observed, modeled negative and positive predictive values were high.

TB presents a framework for diagnosing infections that react after latency. Similar to measuring antibody responses, probing the T cell repertoire serves as a useful adjunctive diagnostic; only people infected with the pathogen harbor T cells reactive to specific antigens. We showed proof of concept for an ELISpot assay measuring T cell responses to *Histoplasma* antigen. Intracellular cytokine staining using FISH-Flow, which has been used to measure reactive T cell populations for *M. tuberculosis* (23, 43), document IFN- $\gamma$  production at the mRNA level, corresponding to protein expression by ELISA and ELISpot. These data support the conclusion that Ag-specific cytokine secretion represents Ag-specific

T-memory responses (44). Two cases examined by FISH-Flow show antigen-specific stimulation of a memory T cell population consistent with Th1 protective immunity after primary infection (45). Prominent Ag-specific TNF- $\alpha$  and IL-17 responses were also observed in a case subject who was 1 year after treatment of subacute disease, consistent with previous characterizations of protective immunity (46–48). Noninfected controls did not produce IFN- $\gamma$ , consistent with a lack of reactive Ag-specific T cell populations; increased IL-2 production by control T cells (2-fold) is less robust than that in the case with documented infection (4-fold) and is likely to represent nonspecific stimulation of responding cells by polysaccharides present within the crude antigen preparation.

There are several limitations to these data. Although standardized definitions were used, it is difficult to identify ‘true controls’ because the organism is endemic in a large swath of American geography and infection can be asymptomatic, self-limited, and undocumented in healthy people. Histoplasmosis causes a wide variety of clinical manifestations and, as in serology, assay responses are likely to vary according to syndrome and timing relative to infection. This assay used a crude antigen preparation prepared from whole yeast extract, thus containing both inflammatory polysaccharides ( $\beta$ -glucan) and fungal proteins. Although we saw only small differences in paired responses in the small number of subjects studied, strain choice may be important, as North American species differ in both glucan composition and gene expression, potentially conferring specificity toward autochthonous responses (49, 50). Further studies will be necessary to optimize antigen preparation and understand the amount of cross-reactivity conferred by other endemic mycoses, especially given the limited geographic variability represented in this proof-of-concept study. Development of recombinant antigen preparations may assist both sensitivity and specificity of IGRAs for endemic fungal infections.

When performance was calculated using the entire cohort of people, which included healthy volunteers, in a region of hyperendemicity, specificity decreased to 79%. This likely represents unrecognized latent infection among healthy people, although other causes of false positivity, including antigen cross-reactivity, cannot be ruled out. Adapting this test for evaluation of latent infection may enable more accurate screening to prevent histoplasmosis disease reactivation after immunosuppressive biological therapies and/or to inform diagnostic differentials. Two studies have shown that recognition of latent histoplasmosis by integration of serologic testing in diagnostic algorithm of pulmonary nodules enable fewer unnecessary surgeries in regions of endemicity (51, 52). Because the geographical distribution of this organism has spread beyond classic areas of exposure in North America (17, 24), ELISpot technology may also prove valuable in reassessing the global epidemiology of *Histoplasma* infection.

## ACKNOWLEDGMENTS

Financial support for a portion of these studies was provided by the JHU Fisher Center (K.A.M.) and NIH AI no. 106036 (Y.B.).

Preliminary data were presented at ASM Microbe 2017 (New Orleans, LA, abstract no. 4185) and MSGERC 2022 (Albuquerque, NM).

K.A.M. reports issuance of the US patent (no. US-10107822-B2) describing the HistoSPOT technology, licensed by Pearl Diagnostics, Inc. (Baltimore, MD). K.D. reports employment income from Pearl Diagnostics at the time of manuscript preparation. K.A.M. reports income from Sfunga Therapeutics and equity in Pearl Diagnostics. N.P. has received grants and salary support from the Health Systems Research Institute (Thailand), the Fisher Center Discovery Program (JHU), the Cystic Fibrosis Foundation, the National Institutes of Health, CareDx, and Merck outside the submitted work, and served on the Advisory Board for Shionogi Inc. and the Data Review Committee for Pulmocide Ltd. S.M.S. reports consultancy income from Pearl Diagnostics. Y.B. holds US (no. US-10900072-B2) and EU patents (no. EP3828278A1) covering FISH-Flow but reports no income from said patents. R.L., S.D., and J.N. report no conflicts of interest.

## REFERENCES

- Ajello L. 1964. Relationship of *Histoplasma capsulatum* to avian habitats. Public Health Rep (1896) 79:266–270. <https://doi.org/10.2307/4592099>.
- Queiroz-Telles F, Fahal AH, Falci DR, Caceres DH, Chiller T, Pasqualotto AC. 2017. Neglected endemic mycoses. Lancet Infect Dis 17:e367–e377. [https://doi.org/10.1016/S1473-3099\(17\)30306-7](https://doi.org/10.1016/S1473-3099(17)30306-7).
- Eissenberg LG, Goldman WE. 1991. *Histoplasma* variation and adaptive strategies for parasitism: new perspectives on histoplasmosis. Clin Microbiol Rev 4:411–421. <https://doi.org/10.1128/CMR.4.4.411>.
- Baker J, Kosmidis C, Rozaliyani A, Wahyuningsih R, Denning DW. 2020. Chronic pulmonary histoplasmosis—a scoping literature review. Open Forum Infect Dis 7:ofaa119. <https://doi.org/10.1093/ofid/ofaa119>.
- Rippon JW. 1988. Histoplasmosis, p 381–423. In Rippon JW (ed), Medical mycology: pathogenic fungi and pathogenic actinomycetes, 3rd ed. WB Saunders, Philadelphia, PA.
- Wood KL, Hage CA, Knox KS, Kleiman MB, Sannuti A, Day RB, Wheat LJ, Twigg HL, 3rd. 2003. Histoplasmosis after treatment with anti-tumor necrosis factor- $\alpha$  therapy. Am J Respir Crit Care Med 167:1279–1282. <https://doi.org/10.1164/rccm.200206-563OC>.
- Azar MM, Hage CA. 2017. Laboratory diagnostics for histoplasmosis. J Clin Microbiol 55:1612–1620. <https://doi.org/10.1128/JCM.02430-16>.
- Azar MM, Hage CA. 2017. Clinical perspectives in the diagnosis and management of histoplasmosis. Clin Chest Med 38:403–415. <https://doi.org/10.1016/j.ccm.2017.04.004>.
- Hage CA, Ribes JA, Wengenack NL, Baddour LM, Assi M, McKinsey DS, Hammoud K, Alapat D, Babady NE, Parker M, Fuller D, Noor A, Davis TE, Rodgers M, Connolly PA, El Haddad B, Wheat LJ. 2011. A multicenter evaluation of tests for diagnosis of histoplasmosis. Clin Infect Dis 53:448–454. <https://doi.org/10.1093/cid/cir435>.
- Hage CA, Wheat LJ. 2010. Diagnosis of pulmonary histoplasmosis using antigen detection in the bronchoalveolar lavage. Expert Rev Respir Med 4:427–429. <https://doi.org/10.1586/ers.10.36>.
- Falci DR, Hoffmann ER, Paskulin DD, Pasqualotto AC. 2017. Progressive disseminated histoplasmosis: a systematic review on the performance of non-culture-based diagnostic tests. Braz J Infect Dis 21:7–11. <https://doi.org/10.1016/j.bjid.2016.09.012>.
- Caceres DH, Knuth M, Derado G, Lindsley MD. 2019. Diagnosis of progressive disseminated histoplasmosis in advanced HIV: a meta-analysis of assay analytical performance. J Fungi (Basel) 5:76. <https://doi.org/10.3390/jof5030076>.
- Richer SM, Smedema ML, Durkin MM, Herman KM, Hage CA, Fuller D, Wheat LJ. 2016. Improved diagnosis of acute pulmonary histoplasmosis by combining antigen and antibody detection. Clin Infect Dis 62: 896–902. <https://doi.org/10.1093/cid/ciw007>.
- Bloch KC, Myint T, Raymond-Guillen L, Hage CA, Davis TE, Wright PW, Chow FC, Woc-Colburn L, Khairy RN, Street AC, Yamamoto T, Albers A, Wheat LJ. 2018. Improvement in diagnosis of *Histoplasma* meningitis by combined testing for histoplasma antigen and immunoglobulin G and immunoglobulin M anti-*Histoplasma* antibody in cerebrospinal fluid. Clin Infect Dis 66:89–94. <https://doi.org/10.1093/cid/cix706>.
- Swartzentruber S, LeMonte A, Witt J, Fuller D, Davis T, Hage C, Connolly P, Durkin M, Wheat LJ. 2009. Improved detection of *Histoplasma* antigenemia following dissociation of immune complexes. Clin Vaccine Immunol 16:320–322. <https://doi.org/10.1128/CI.00409-08>.
- Naeem F, Metzger ML, Arnold SR, Adderson EE. 2015. Distinguishing benign mediastinal masses from malignancy in a histoplasmosis-endemic region. J Pediatr 167:409–415. <https://doi.org/10.1016/j.jpeds.2015.04.066>.
- Benedict K, Beer KD, Jackson BR. 2020. Histoplasmosis-related healthcare use, diagnosis, and treatment in a commercially insured population, United States. Clin Infect Dis 70:1003–1010. <https://doi.org/10.1093/cid/ciz324>.
- Toscanini MA, Barberis F, Benedetti MF, Garrido AV, Posse GB, Capece P, Daneri GL, Nusblat AD, Cuestas ML. 2022. Detection of anti-*Histoplasma capsulatum* antibodies and seroconversion patterns in critically ill patients with COVID-19: an underdiagnosed fungal entity complicating COVID-19? Med Mycol 60:myac012. <https://doi.org/10.1093/mmy/myac012>.
- Ferreira SDC, Nobrega FJF, de Araujo RC, de Almeida PH, Villanova MG, Santana RC, Zambelli Ramalho LN, Martinelli ALC, Troncon LEA. 2021. Histoplasmosis related to immunosuppression in a patient with Crohn's disease: a diagnostic challenge. Am J Case Rep 22:e925345. <https://doi.org/10.12659/AJCR.925345>.
- De Pauw B, Walsh TJ, Donnelly JP, Stevens DA, Edwards JE, Calandra T, Pappas PG, Maertens J, Lortholary O, Kauffman CA, Denning DW, Patterson TF, Maschmeyer G, Bille J, Dismukes WE, Herbrecht R, Hope WW, Kibbler CC, Kullberg BJ, Marr KA, Munoz P, Odds FC, Perfect JR, Restrepo A, Ruhnke M, Segal BH, Sobel JD, Sorrell TC, Viscoli C, Wingard JR, Zaoutis T, Bennett JE. 2008. Revised definitions of invasive fungal disease from the European Organization for Research and Treatment of Cancer/Invasive Fungal Infections Cooperative Group and the National Institute of Allergy and Infectious Diseases Mycoses Study Group (EORTC/MSG) Consensus Group. Clin Infect Dis 46: 1813–1821. <https://doi.org/10.1086/588660>.
- Armstrong PA, Jackson BR, Haselow D, Fields V, Ireland M, Austin C, Signs K, Fialkowski V, Patel R, Ellis P, Iwen PC, Pedati C, Gibbons-Burgener S, Anderson J, Dobbs T, Davidson S, McIntyre M, Warren K, Midia J, Luong N, Benedict K. 2018. Multistate epidemiology of histoplasmosis, United States, 2011–2014. Emerg Infect Dis 24:425–431. <https://doi.org/10.3201/eid2403.171258>.
- Teixeira MdM, Patané JSL, Taylor ML, Gómez BL, Theodoro RC, de Hoog S, Engelthaler DM, Zancopé-Oliveira RM, Felipe MSS, Barker BM. 2016. Worldwide phylogenetic distributions and population dynamics of the genus *Histoplasma*. PLoS Negl Trop Dis 10:e0004732. <https://doi.org/10.1371/journal.pntd.0004732>.
- Arrigucci R, Bushkin Y, Radford F, Lakehal K, Vir P, Pine R, Martin D, Sugarman J, Zhao Y, Yap GS, Lardizabal AA, Tyagi S, Gennaro ML. 2017. FISH-Flow, a protocol for the concurrent detection of mRNA and protein in single cells using fluorescence *in situ* hybridization and flow cytometry. Nat Protoc 12:1245–1260. <https://doi.org/10.1038/nprot.2017.039>.
- McKinsey DS, Pappas PG. 2019. Histoplasmosis: time to redraw the map and up our game. Clin Infect Dis 70:1011–1013. <https://doi.org/10.1093/cid/ciz327>.
- Falci DR, Monteiro AA, Braz Caurio CF, Magalhaes TCO, Xavier MO, Basso RP, Melo M, Schwarzbald AV, Ferreira PRA, Vidal JE, Marochi JP, Godoy CSM, Soares RBA, Paste A, Bay MB, Pereira-Chiccola VL, Damasceno LS, Leitao T, Pasqualotto AC. 2019. Histoplasmosis, an underdiagnosed disease affecting people living with HIV/AIDS in Brazil: results of a multicenter prospective cohort study using both classical mycology tests and *Histoplasma* urine antigen detection. Open Forum Infect Dis 6:ofz073. <https://doi.org/10.1093/ofid/ofz073>.
- Gailey MP, Klutts JS, Jensen CS. 2013. Fine-needle aspiration of histoplasmosis in the era of endoscopic ultrasound and endobronchial ultrasound: cytomorphologic features and correlation with clinical laboratory testing. Cancer Cytopathol 121:508–517. <https://doi.org/10.1002/cncy.21298>.
- Weydert JA, Van Natta TL, DeYoung BR. 2007. Comparison of fungal culture versus surgical pathology examination in the detection of *Histoplasma* in surgically excised pulmonary granulomas. Arch Pathol Lab Med 131:780–783. <https://doi.org/10.5858/2007-131-780-COFCVS>.
- Oladele RO, Ayanlowo OO, Richardson MD, Denning DW. 2018. Histoplasmosis in Africa: an emerging or a neglected disease? PLoS Negl Trop Dis 12:e0006046. <https://doi.org/10.1371/journal.pntd.0006046>.
- Mahto SK, Jamal A, Gupta PK, Majumdar P, Grewal V, Agarwal N. 2019. A rare cause of nodular skin lesions with fever in an immunocompetent individual. J Family Med Prim Care 8:1287–1289. [https://doi.org/10.4103/jfmpc.jfmpc\\_26\\_19](https://doi.org/10.4103/jfmpc.jfmpc_26_19).
- Ling Q, Zhu W, Lu Q, Jin T, Ding S. 2018. Disseminated histoplasmosis in an immunocompetent patient from an endemic area: a case report. Medicine (Baltimore) 97:e11486. <https://doi.org/10.1097/MD.00000000000011486>.
- Baadhya NK, Jadon RS, Mondal S, Vikram NK, Sood R. 2018. Progressive disseminated histoplasmosis in an immunocompetent adult: a case report. Intractable Rare Dis Res 7:126–129. <https://doi.org/10.5582/irdr.2018.01022>.
- Ghosh R, Mishra P, Sen S, Maiti PK, Chatterjee G. 2016. Experience of varied presentation of chronic progressive disseminated histoplasmosis in immunocompetent patients: a diagnostic conundrum. Indian J Dermatol 61:580. <https://doi.org/10.4103/0019-5154.190128>.
- Raina RK, Mahajan V, Sood A, Saurabh S. 2016. Primary cutaneous histoplasmosis in an immunocompetent host from a nonendemic area. Indian J Dermatol 61:467. <https://doi.org/10.4103/0019-5154.185748>.
- Rihana NA, Kandula M, Velez A, Dahal K, O'Neill EB. 2014. Histoplasmosis presenting as granulomatous hepatitis: case report and review of the literature. Case Rep Med 2014:879535. <https://doi.org/10.1155/2014/879535>.
- Kash N, Jahan-Tigh RR, Efron-Everett M, Vigneswaran N. 2014. Primary mucocutaneous histoplasmosis in an immunocompetent patient. Dermatol Online J 21:13030/qt87614080.
- Rahman MT, Bakar NH, Philip R, Shamsudin AR. 2004. Oral histoplasmosis presenting as oral ulcer in a non-HIV patient. Southeast Asian J Trop Med Public Health 35:388–390.
- Hott JS, Horn E, Sonntag VK, Coons SW, Shetter A. 2003. Intramedullary histoplasmosis spinal cord abscess in a nonendemic region: case report and review of the literature. J Spinal Disord Tech 16:212–215. <https://doi.org/10.1097/00024720-200304000-00016>.



38. Sanguino JC, Rodrigues B, Baptista A, Quina M. 1996. Focal lesion of African histoplasmosis presenting as a malignant gastric ulcer. *Hepatogastroenterology* 43:771–775.
39. Ramireddy S, Wanger A, Ostrosky L. 2012. An instructive case of CNS histoplasmosis in an immunocompetent host. *Med Mycol Case Rep* 1:69–71. <https://doi.org/10.1016/j.mmcr.2012.08.002>.
40. Urschel HC, Jr., Razzuk MA, Netto GJ, Disiere J, Chung SY. 1990. Sclerosing mediastinitis: improved management with histoplasmosis titer and ketoconazole. *Ann Thorac Surg* 50:215–221. [https://doi.org/10.1016/0003-4975\(90\)90737-Q](https://doi.org/10.1016/0003-4975(90)90737-Q).
41. Wheat LJ, Freifeld AG, Kleiman MB, Baddley JW, McKinsey DS, Loyd JE, Kauffman CA, Infectious Diseases Society of America. 2007. Clinical practice guidelines for the management of patients with histoplasmosis: 2007 update by the Infectious Diseases Society of America. *Clin Infect Dis* 45: 807–825. <https://doi.org/10.1086/521259>.
42. Rubio-Carrasquilla M, Santa CD, Rendon JP, Botero-Garcés J, Guimaraes AJ, Moreno E, Cano LE. 2019. An interferon gamma release assay specific for *Histoplasma capsulatum* to detect asymptomatic infected individuals: a proof of concept study. *Med Mycol* 57:724–732. <https://doi.org/10.1093/mmy/myy131>.
43. Arriguicci R, Lakehal K, Vir P, Handler D, Davidow AL, Herrera R, Estrada-Guzman JD, Bushkin Y, Tyagi S, Lardizabal AA, Gennaro ML. 2018. Active tuberculosis is characterized by highly differentiated effector memory Th1 cells. *Front Immunol* 9:2127. <https://doi.org/10.3389/fimmu.2018.02127>.
44. Salgame P, Geadas C, Collins L, Jones-Lopez E, Ellner JJ. 2015. Latent tuberculosis infection: revisiting and revising concepts. *Tuberculosis (Edinb)* 95:373–384. <https://doi.org/10.1016/j.tube.2015.04.003>.
45. Allendorfer R, Brunner GD, Deepe GS, Jr. 1999. Complex requirements for nascent and memory immunity in pulmonary histoplasmosis. *J Immunol* 162:7389–7396.
46. Wang H, LeBert V, Hung CY, Galles K, Saijo S, Lin X, Cole GT, Klein BS, Wuthrich M. 2014. C-type lectin receptors differentially induce Th17 cells and vaccine immunity to the endemic mycosis of North America. *J Immunol* 192: 1107–1119. <https://doi.org/10.4049/jimmunol.1302314>.
47. Deepe GS, Jr., Gibbons RS. 2009. Interleukins 17 and 23 influence the host response to *Histoplasma capsulatum*. *J Infect Dis* 200:142–151. <https://doi.org/10.1086/599333>.
48. Deepe GS, Jr., Gibbons RS. 2006. T cells require tumor necrosis factor- $\alpha$  to provide protective immunity in mice infected with *Histoplasma capsulatum*. *J Infect Dis* 193:322–330. <https://doi.org/10.1086/498981>.
49. Rappleye CA, Eissenberg LG, Goldman WE. 2007. *Histoplasma capsulatum*  $\alpha$ -(1,3)-glucan blocks innate immune recognition by the  $\beta$ -glucan receptor. *Proc Natl Acad Sci U S A* 104:1366–1370. <https://doi.org/10.1073/pnas.0609848104>.
50. Edwards JA, Chen C, Kemski MM, Hu J, Mitchell TK, Rappleye CA. 2013. Histoplasma yeast and mycelial transcriptomes reveal pathogenic-phase and lineage-specific gene expression profiles. *BMC Genomics* 14:695. <https://doi.org/10.1186/1471-2164-14-695>.
51. Deppen SA, Massion PP, Blume J, Walker RC, Antic S, Chen H, Durkin MM, Wheat LJ, Grogan EL. 2019. Accuracy of a novel histoplasmosis enzyme immunoassay to evaluate suspicious lung nodules. *Cancer Epidemiol Biomarkers Prev* 28:321–326. <https://doi.org/10.1158/1055-9965.EPI-18-0169>.
52. Shipe ME, Deppen SA, Sullivan S, Kammer M, Starnes SL, Wilson DO, Massion PP, Grogan EL. 2021. Validation of histoplasmosis enzyme immunoassay to evaluate suspicious lung nodules. *Ann Thorac Surg* 111:416–420. <https://doi.org/10.1016/j.athoracsur.2020.05.101>.